Electronic Supplementary Information For:

Controlled Preparation of CdS Nanoparticle Arrays in Amphiphilic Perylene Tetracarboxylic Diimides: Organization, Electron-Transfer and Semiconducting Properties

Jingang Song,[a] Qingwen Tian,[a] Jian Gao,[a] Haixia Wu,[b] Yanli Chen*[a] and Xiyou Li*[b]

[a] *Shandong Provincial Key Laboratory of Fluorine Chemistry and Chemical Materials, School of Chemistry and Chemical Engineering, University of Jinan, Jinan, 250022, China.*
[b] *Department of Chemistry, Shandong University, Jinan,250100, China.*

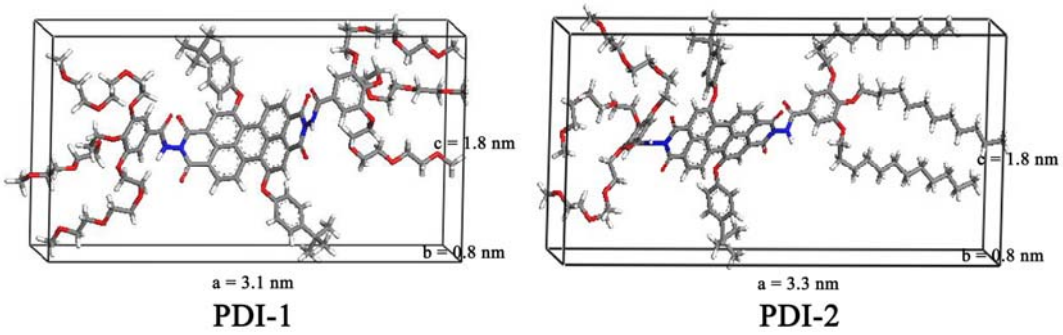

Scheme S1. The energy-optimized conformation of **PDI-1** (left) and **PDI-2 (**right) obtained from DFT calculation (B3LYP/6-31G(d)).

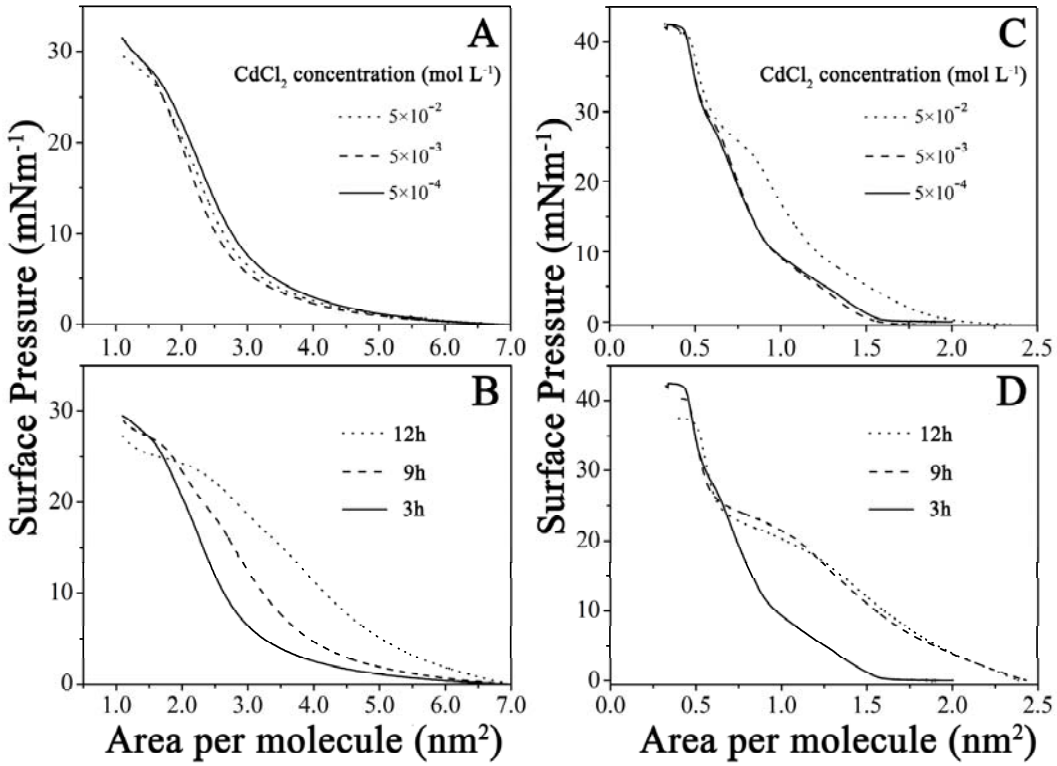

Fig. S1. π-*A* isotherms of the **PDI-1**(A) and **PDI-2** (C) at the air/$CdCl_2$ subphase interface with different $CdCl_2$ concentration after evaporation of CH_2Cl_2 for 3 h; and π-*A* isotherms of the **PDI-1** (B) and **PDI-2** (D) at the air/$CdCl_2$ subphase interface with different interaction time between the PDI molecules and Cd^{2+} ions in the 5×10^{-4} mol L^{-1} $CdCl_2$ subphase.

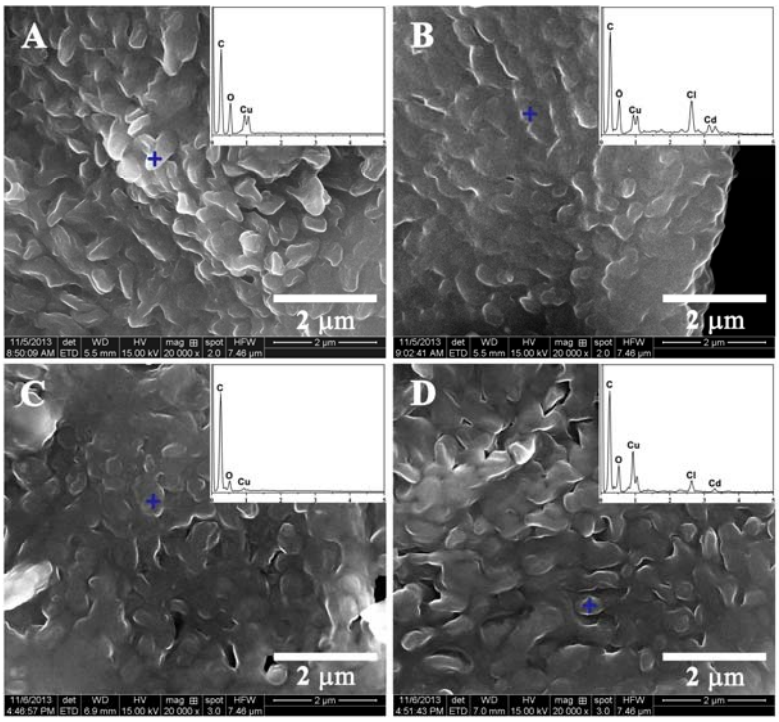

Fig. S2. SEM images of the Langmuir film of the **PDI-1** (top) and **PDI-2** (bottom) on the pure water surface (A and C) and $CdCl_2$ subphase surface (B and D). The inset of A-D shows the EDS pattern collected from the nanoparticle (cross mark) in the corresponding Langmuir films, respectively.

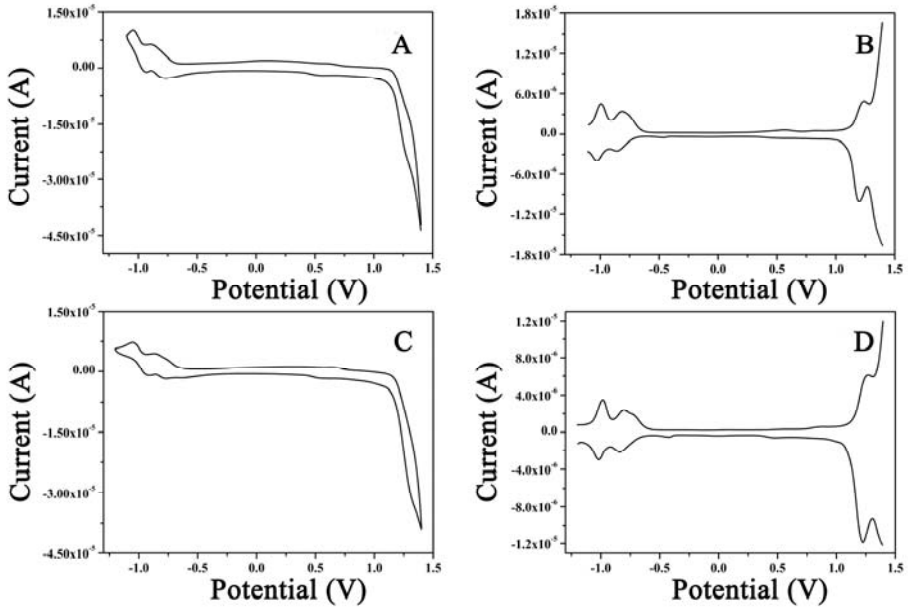

Fig. S3. Cyclic voltammogram (A and C) and differential pulse voltammogram (B and D) of **PDI-1** and **PDI-2**, respectively, in CH_2Cl_2 containing 0.1 M $[NBu_4][ClO_4]$ at a scan rate of 20 and 10 $mV \cdot S^{-1}$.

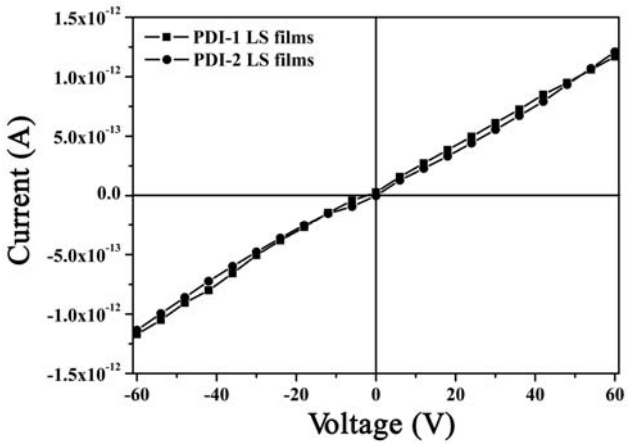

Fig. S4. *I-V* curves of the **PDI-1** and **PDI-2** LS films.

Table S1. The experimental data of X-ray diffraction from **PDI** LS films and CdS/**PDI** composite films.

films	component	2θ / degree	d /nm	hkl or attribution
PDI-1 LS films	**PDI-1**	5.72	1.55	(001)
		28.94	0.31	π-π interaction
	PDI-1	6.04	1.46	(001)
		21.08	0.42	liquid-like ordered packing of long alky chains
		28.94	0.31	π-π interaction
CdS/**PDI-1** composite films	CdS	24.86	0.358	(100)
		26.45	0.357	(002)
		28.22	0.316	(101)
		43.78	0.207	(110)
		51.70	0.177	(112)
PDI-2 LS films	**PDI-2**	3.02	2.92	(001)
		6.02	1.47	(002)
		21.32	0.42	liquid-like ordered packing of long alky and/or alkyl chains
		28.06	0.31	π-π interaction
	PDI-2	4.20	2.10	(001)
		21.08	0.42	liquid-like ordered packing of long alky and/or alkyl chains
		28.02	0.31	π-π interaction
CdS/**PDI-2** composite films	CdS	24.86	0.358	(100)
		26.45	0.357	(002)
		28.22	0.316	(101)
		43.70	0.207	(110)
		52.04	0.176	(112)

Table S2. Half-wave redox potentials of **PDI-1** and **PDI-2** (V vs SCE) in CH_2Cl_2 containing 0.1M TBAP and the HOMO, LUMO levels of **PDI**.

Compound	Oxd_1 (V) [b]	Red_1 (V) [b]	Red_2 (V) [b]	E_{HOMO}(eV) [c]	E_{HOMO} (eV) [c]	$\triangle E^o_{1/2}$ (V) [a]
PDI-1	1.52	-0.54	-0.71	-5.96	-3.90	2.05
PDI-2	1.54	-0.53	-0.70	-5.98	-3.95	2.07

[a] $\triangle E^o_{1/2} = Oxd_1 - Red_1$, i.e. the HOMO-LUMO gap of corresponding molecule.

[b] Recorded by DPV.

[c] Calculated from empirical formula[1]: HOMO = -(Oxd_1+4.44 eV).

[d] LUMO = −(Red_1+4.44 eV).

Table S3. The experimental data of fluorescence decay（τ）from **PDI** LS films and CdS/**PDI** composite films.

τ/ns	pure LS films	CdS/**PDI** composite films		
		40 nm	60 nm	80 nm
PDI-1	2.91	1.20 (88.76%)	1.30 (86.03%)	1.57 (89.87%)
		11.24 (11.24%)	10.99 (13.97%)	10.10 (10.13%)
		20 nm	30 nm	
PDI-2	3.50	1.40 (91.98%)	2.50 (82.19%)	
		17.30 (8.02%)	10.20 (17.81%)	

1. S. Vajiravelu, L. Ramunas, G. J. Vidas, G. Valentas,; J. Vygintas, S. Valiyaveettil. *J. Mater. Chem.* 2009, **19**, 4268.